RESEARCH   **Open Access**

Research on Angle Connector in Composite Beam

Kewei Ding[1*] , Xinqi Zhang[1], Yunlin Liu[1], Shulin He[1], Jingfeng Wang[2] and Wanyu Shen[3]

Abstract

As a critical component for steel beam and concrete slab to work together, the strength of the shear connector affects the flexural load capacity and stiffness of the composite beam. Connectors were generally studied for longitudinal shear resistance. However, transverse shear needs to be considered when the main beam is far away and the transverse connection is weak. In this paper, an angle connector pre-embedded in the precast slab was proposed, and its pre-embedded position makes it exhibit better transverse shear resistance. To assess the strength, stiffness, and slip capacity of the angle connector, two groups of composite beam with precast slabs negative moment flexural were tested, then several finite element groups were simulated in push-out test. The test variable was the existence of angle connectors, and the variables simulated were the yield strength of the angle connector and its flange thickness. The results showed that the composite beam with angle connectors has greater stiffness than ordinary ones, with little difference in flexural strength capacity and less slippage. The results show that angle connectors can replace extending rebars in precast slabs, which will reduce construction costs. In addition, a new design equation was proposed, including the yield strength of the connector and the thickness of its flange which are not unified in the current equations. The simulations determined the strength of the angle connectors in relation to the yield strength of the angle connector and its web thickness.

Keywords: composite beam with precast slabs, angle connector, shear strength, finite element model, flexural test

1 Introduction

The steel–concrete composite beam is made of steel beam and concrete slab connected by shear connectors. It has the structural advantage of combining two materials into one and provides the advantages of high stiffness, high flexural capacity, and easy construction (Liu, 2017; Sahu & Das, 2020). As a type of composite beam, composite beam with precast slabs has good application prospects because of its advantages such as excellent stress performance and convenient construction (Ding et al., 2015; Liu et al., 2014; Nie & Yu, 1999). The rebars of the precast slabs extend outward to improve the overall performance, however, it makes transportation and installation inconvenient. This raises the cost of the project and is not conducive to its widespread use.

As part of the steel beam and concrete slab working together, the connectors are required to resist both longitudinal and transverse shear forces between steel beam and concrete slab. The study generally focuses on longitudinal shear forces (Paknahad et al., 2018; Shariati et al., 2012). Some scholars have conducted a more systematic study on the behavior of angle connector at high temperatures (Davoodnabi et al., 2019, 2021; Nouri et al., 2021; Shahabi et al., 2016; Shariati et al., 2021). To save costs, soft computing has been used to predict the shear capacity of angle connectors with accurate results (Chahnasir et al., 2018; Safa et al., 2016; Sedghi et al., 2018; Shariati et al., 2019; Shariati et al., 2021; Toghroli et al., 2014). Evaluation of the behaviour of angle connectors in high strength and light weight concrete (Shariati et al., 2010a, b, 2011a, b, 2012, 2016a). There are few studies

---

*Correspondence: dingkw@ahjzu.edu.cn
[1] College of Civil Engineering, Anhui Jianzhu University, Hefei 230601, Anhui, China
Full list of author information is available at the end of the article

on transverse shear of composite beams. However, when the distance of the main beam is large and the transverse connection of the main beam is weak, the transverse shear capacity of the connector should not be neglected as well (JTG/T D64-01-2015, 2015). In this case, the connectors must provide sufficient transverse loading to ensure structural safety. This requires the shear and pull-out forces of the connectors to resist the transverse shear forces. Therefore, it will be necessary and meaningful to study the transverse shear resistance in the composite beam.

The form of the connection is critical to the impact of the concrete structure (Ding et al., 2021). In composite beam structures, studs are the most commonly used shear connectors. However, the amount of studs required in composite beams is large and the welding process has high requirements. Compared to studs, channel, angle and V-shaped angle connectors have a higher load capacity and no extra inspections are required. In addition, angle connectors as shear connections have the advantage of using less steel and simple welding (Liu et al., 2016; Shariati et al., 2013; Shariati et al., 2016). The study of angle connections in composite beams will be more beneficial to the wider use of composite beams. Fig. 1 shows a pre-embedded angle connector designed in this paper, which was pre-embedded in the precast slab of the composite beam.

Connections located in the negative moment zone are weaker constrained by the surrounding concrete than by compression. In addition, the connector in the negative moment zone is mainly subjected to shear and pull-out forces, and its shear resistance is weakened (GB/T50017-2017, 2017). However, the shear resistance of the connector directly affects the overall performance of the precast and cast-in-place slabs (Nie et al., 2003). Thus, it will directly affect the performance of the composite beam. Therefore, it is necessary to study the overall performance of composite beams with precast slabs under negative bending moments to ensure the safe use of the members.

In this paper, we proposed an angle connector that is pre-embedded in the precast slab. Simplify construction by pre-embedding this connector instead of the traditional rebars extending out of the precast slab. In addition, this connector can provide transverse shear, which will be a complement to the transverse shear content of the composite beam. The new design equation is proposed for the different forms and differences in the strength design equations of angle connectors at domestic and foreign. The equation takes into account the yield strength of the connector and its flange thickness, which is not unified by the previous equation.
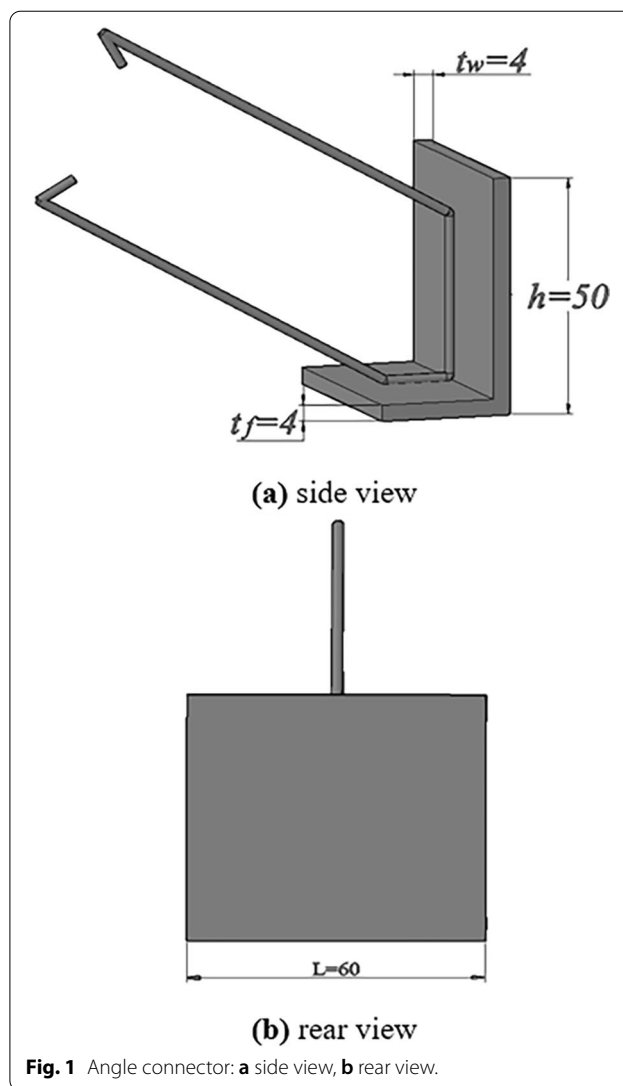

Fig. 1 Angle connector: **a** side view, **b** rear view.

To investigate whether composite beam with angle connectors can be used safely under negative bending moment conditions so as to replace conventional composite beams and make construction easier. Two sets of flexural tests on composite beam with precast slabs were conducted. The variables tested were the presence or absence of the angle connectors. Due to its obvious shear orientation, the transverse shear performance of the angle connectors was evaluated by ABAQUS finite element software for transverse push-out test simulations. In addition, the connector yield strength and flange thickness were used as variables to study the strength of the connector.
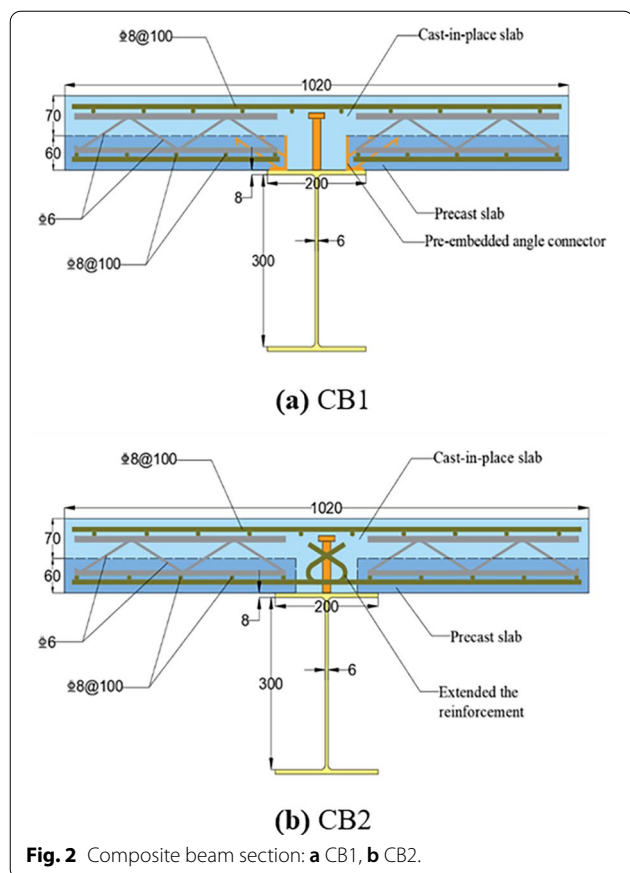
Ding *et al. Int J Concr Struct Mater*   (2022) 16:15

Page 3 of 16

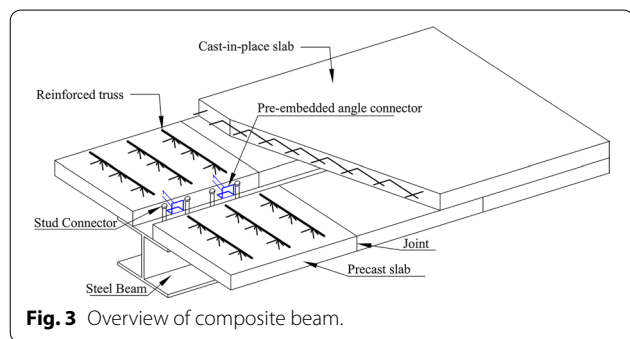**Fig. 2** Composite beam section: **a** CB1, **b** CB2.

Fig. 3 Overview of composite beam.

2 Test Program

2.1 Specimen Design

In this paper, two sets of full-size composite beam specimens with precast slabs, CB1 and CB2, were designed, and the variables for both sets of tests were the presence or absence of angle connectors. Fig. 2 shows a cross-sectional view of CB1 and CB2, the cross-sectional size of the precast slab is 450×60 mm, and the length of each precast slab placed on the steel beam is 40 mm. The geometry of the test pieces is designed according to the specification (GB/T50017-2017, 2017). Fig. 3 shows a general overview of the composite beam. The length of the precast slab in the long direction of the beam is 1320 mm. In addition, the precast slabs with angle connectors did not have extending rebars to facilitate the construction. All composite beam specimens were made of the same steel beam material and dimensions, and were made of Q235B type hot rolled H-beam. The main parameters of the specimens are given in Table 1.

The total length of the composite beam is 3960 mm and the net span is 3560 mm. The longitudinal and transverse rebars in the slab were HRB400 rebars, and the reinforced trusses were made of 10-mm-diameter upper chord rebars (HRB400), 6 mm web rebars (HRB300), and 8 mm lower chord rebars (HRB400). The concrete used for both precast and cast-in-place slabs was C30, and the thickness of the protective layer was 15 cm. The shear-resistant connectors consist of studs and angle connectors, where the angle connectors are made of Q345B steel. According to code GB/T 10433-2002, the stud specification is M16-100 (16 mm diameter, 100 mm height, 250 mm distance) (GB/T10433-2002, 2002). The dimensions of the angle connectors are based on GB/T 706-2016 (GB/T706-2016, 2016). The length of the angle connector is 60 mm. The distance between angle connector is 500 mm, symmetrically pre-embedded in the precast slab.

2.2 Specimen Preparation

Fig. 4 shows the fabrication process of the composite beam with precast slabs. The precast slab of a single composite beam is made up of six identical small precast slabs in total. The angle connectors are pre-embedded in the precast slab. The cross-sectional dimension of the small precast slab is 450×60 mm and the length is 1020 mm. Small slabs are spliced together with short sides. Four longitudinal rebars with a distance of 130 mm and a length of 1240 mm are placed at each joint. There are 5

Table 1 Main parameters of the specimen.

Specimen	Slab section (mm)	Beam section (mm)	Studs distance (mm)	Angle connector	Extended reinforcement
CB-1	1020×130	$200 \times 316 \times 8 \times 6$	250	With	Without
CB-2	1020×130	$200 \times 316 \times 8 \times 6$	250	Without	With

(a) precast slab production

(b) precast slab placement

(c) welded angle

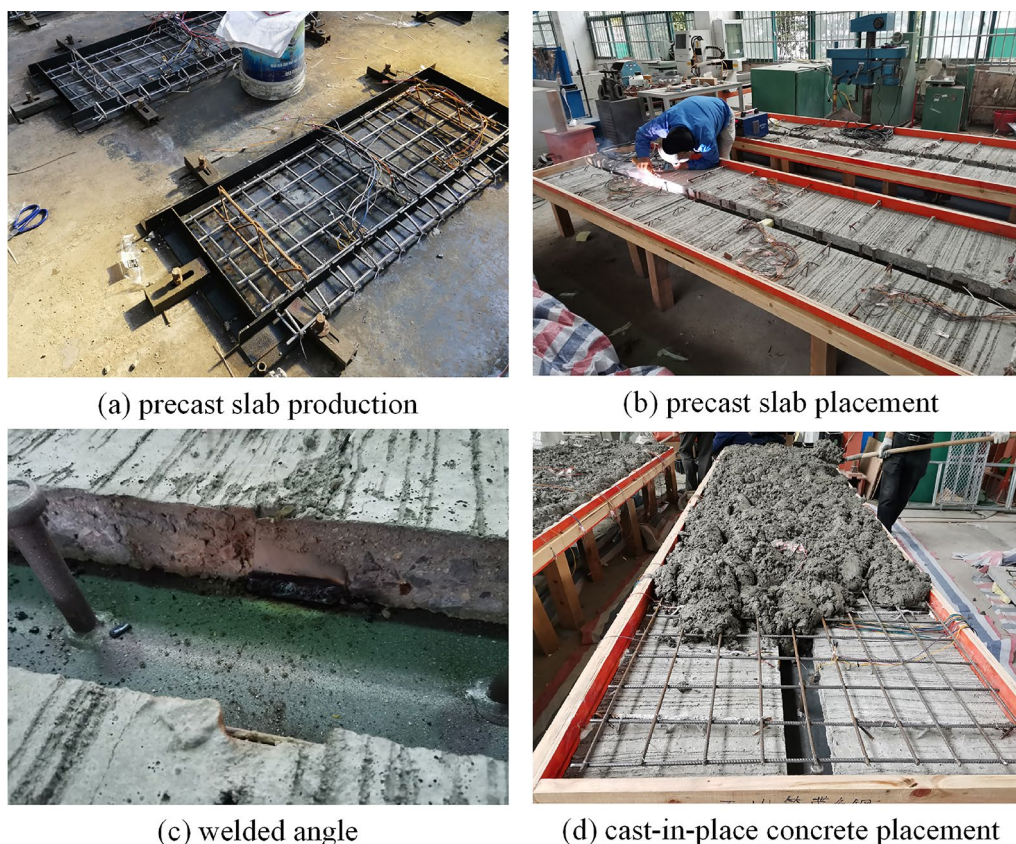(d) cast-in-place concrete placement

Fig. 4 The fabrication process of the composite beam with precast slab: **a** precast slab production, **b** precast slab placement, **c** welded angle, **d** cast-in-place concrete placement.

transverse distribution rebars above the additional rebars at the joints with a distance of 250 mm and a length of 420 mm.

2.3 Material Test

According to the "tensile test of metal materials requirements", there are four groups of material tensile tests, corresponding to different rebars and steel plates. Each group has 3 specimens, among which, the steel beam takes its flange to make tensile specimens. All specimens are completed the tensile test on WDW-100D universal testing machine (GB/T228.1-2010, 2010). Table 2 shows the material properties of the measured steel. Specimens of standard size were made during the casting of concrete for precast slabs and concrete for cast-in-place slabs, and the compressive strengths were 35.6 MPa and 33.2 MPa, respectively (Huang et al., 2021).

2.4 Loading Systems and Measurement Schemes

Fig. 5 shows the loading device, which used hydraulic jacks (500 kN range) to provide a vertical concentrated load on the span of the member. The boundary condition

Table 2 Steel material performance test results.

Categories	Type	f_y (MPa)	f_u (MPa)
Steel beam	Q235B	275	390
6 mm bar	HRB300	452	560
8 mm bar	HRB400	480	660
10 mm bar	HRB400	456	620

of simple support was adopted, and the load is applied at the loading plate, which on the mid-span of the flange of the steel beam. The loading system was force-controlled before yielding with 15kN per level, then system was displacement-controlled after yielding with 5 mm per level, and holding the load for 2 min after each level of loading. Loading until the longitudinal crack width at the main tensile reinforcement reached 1.5 mm, the loading ended (GB/T50152-2012, 2012). The loading rate was 15 kN/min, 2.5 mm/min, respectively.
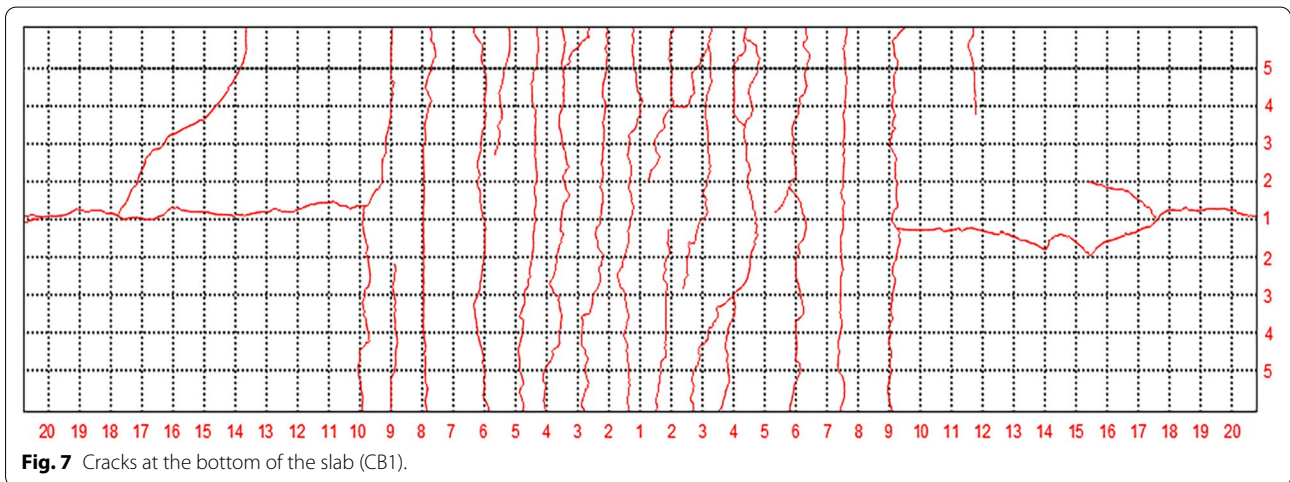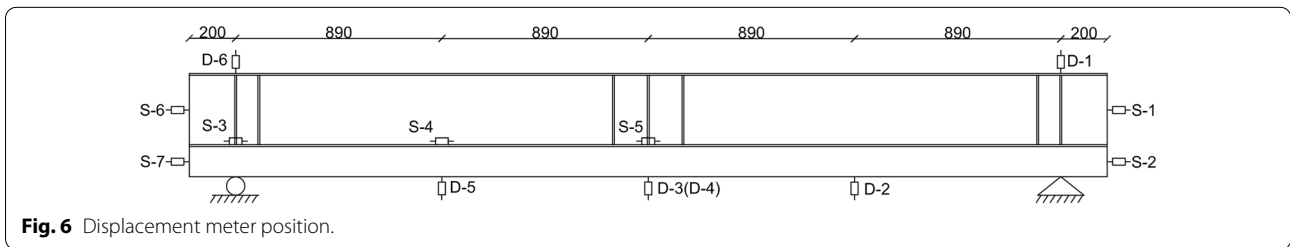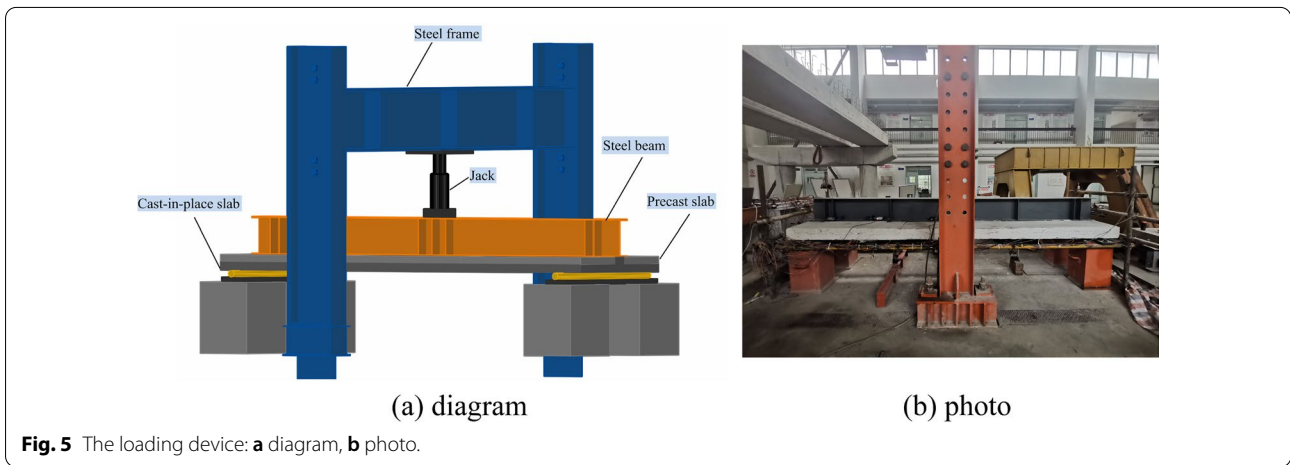
The test measurements included load–displacement, as well as the observation of the development of cracks

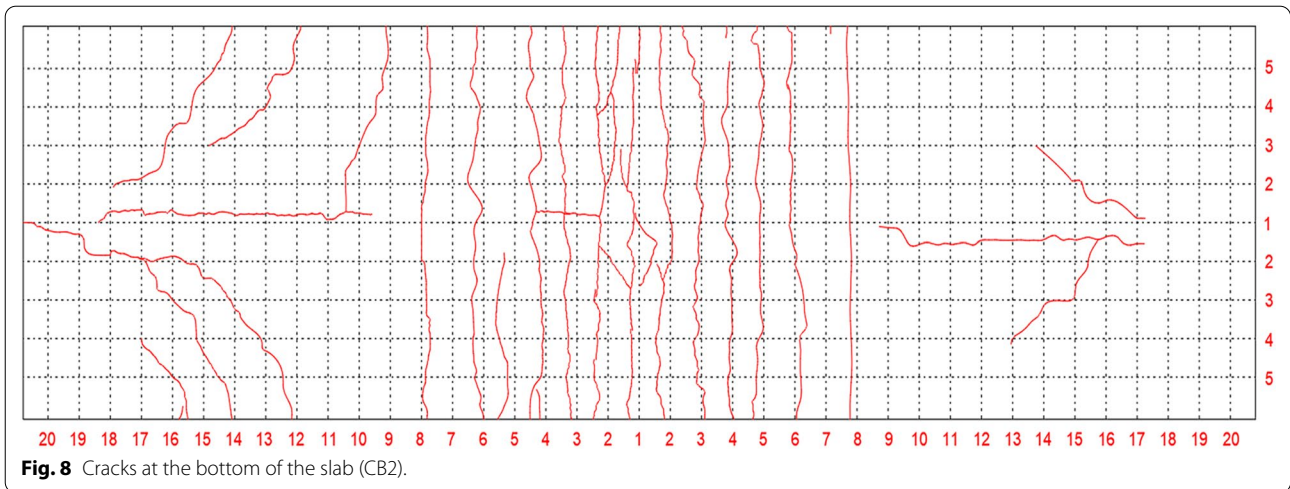Ding *et al. Int J Concr Struct Mater*   (2022) 16:15

Page 5 of 16

in the concrete slab and the damage pattern of the members. Displacement meter positions in Fig. 6, D1–D6 were used for measuring the bending deformation of the composite beam. They were set vertically up the supports, the quarter points at the bottom of the slab, and the middle of the span, respectively. Two of them were placed symmetrically in the middle of the span to take the average value.

3 Experimental Results and Analysis
3.1 Experimental Phenomena and Crack Characteristics
The cracks at the bottom of the two groups of slabs were similar, as shown in Figs. 7 and 8. Due to the presence of slab joints, transverse cracks developed earlier in CB1 and CB2 at 1/3 of the joint along the beam longitudinal direction, and the number of cracks at this location was also larger. Most of the shear diagonal cracks were at the concrete above the stud and angle connectors. When

Fig. 5 The loading device: **a** diagram, **b** photo.

Fig. 6 Displacement meter position.

Fig. 7 Cracks at the bottom of the slab (CB1).

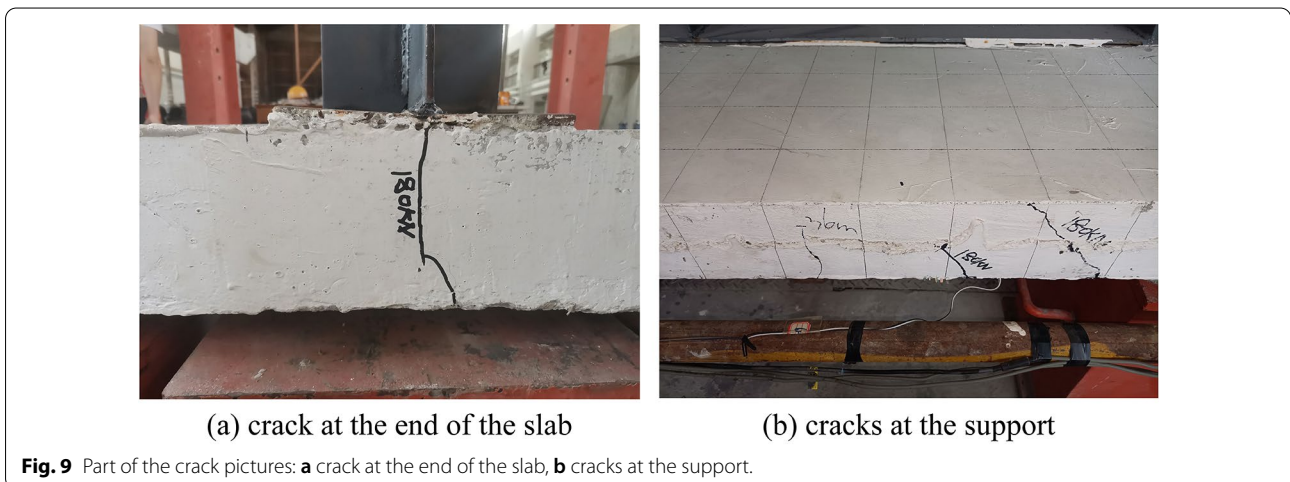**Fig. 8** Cracks at the bottom of the slab (CB2).

the load was increased to 60 kN–76 kN, the first crack appeared at the mid-span of the two specimens. This crack eventually became the fastest developing and the widest "main crack". With the load increased, new cracks kept developing along the length of the slab. At the same time, cracks at the mid-span kept developing and gradually increased in width. Eventually, it developed into a crack through the concrete slab.

Specimen CB1: When the load was increased to $0.2P_u$, the first crack developed at the bottom of the slab joints. The first mid-span crack appeared at the bottom of the slab when the load increased to $0.25P_u$. When loaded to $0.4P_u \sim 0.43P_u$, penetration cracks appeared in the mid-span and at the joints, and these cracks extended to the side of the slab. During the later loading process, new transverse flexural cracks and shear diagonal cracks were continuously developed along the longitudinal direction of the composite beam. When the load was increased to

$0.6P_u$, longitudinal splitting cracks developed along the axis of the studs at both ends of the slab. As shown in Fig. 9, these splitting cracks developed toward the side of the slab end and in the mid-span, and several new shear diagonal cracks developed at the surface of the concrete above the studs. At the same time, diagonal cracks were developed at the supports on the side of the slab. When the load was added to $0.9P_u$, the flange of the steel beam buckled. The stiffness of the member was significantly declined at this moment, with a mid-span displacement of 12.9 mm. Finally, the member was loaded by displacement-controlled. The loading was stopped when the displacement at mid-span reached 18.35 mm, and the load was 296.08 kN.

Specimen CB2: The first crack developed at the bottom of the slab joints when the load was increased to $0.25P_u$. When the load was increased to $0.3P_u$, the first crack developed at the mid-span of the bottom of the slab, and

(a) crack at the end of the slab   (b) cracks at the support

Fig. 9 Part of the crack pictures: **a** crack at the end of the slab, **b** cracks at the support.

the crack at the joints extended to the bottom of the slab. At a load of $0.5P_u$, penetration cracks appeared at the mid-span and the joints. When the load was increased to $0.6P_u$, longitudinal splitting cracks developed along the axis of the studs at both sides of the slab end. These splitting cracks developed towards the side of the slab end and at the middle of the span, developing several new shear diagonal cracks on the concrete surface above the studs. At the same time, diagonal cracks were generated at the supports at the side of the slab. When the load was added to $0.9P_u$, the flange of the steel beam buckled. The stiffness of the member was significantly declined at this point, with a displacement of 12.9 mm at mid-span. Finally, the member was loaded by displacement-controlled. The loading was stopped when the displacement at mid-span reached 23.8 mm, and the load was 296 kN.

During the loading process, the experimental phenomenon of the two specimens was similar. Both of them were typical of bending damage. The main results are shown in Table 3. In the initial stage of loading, the load was mainly transferred by the bond between the rebar and concrete. At this point, there was almost no sliding of the member, and no significant phenomenon was observed in this stage of the experimental loading. When the load was increased to about 130kN, the stiffness of the load–displacement curve started to decrease. It was possible that the bond between them failed and the stud and angle connectors started to function. As the load increased, the slippage became larger and the stiffness of the load–displacement curve became flatter. In addition, local buckling of the flange of the steel beam located below the loading plate occurred. Finally, the crack width at the main tensile reinforcement at the mid-span of the member was so large and the test was stopped. Throughout the test, two groups of concrete slabs showed no cracks out of both the old and new laminated surfaces. This indicates that angle connectors can have the same overall performance compared to traditional laminate slabs. Since CB1 has angles, its shear connection is higher than that of CB2. Therefore, the maximum slippage of CB1 was smaller than that of CB2. When the load reached $0.8P_u$, the slippages of CB1 and CB2 were 0.183 mm, 0.354 mm, respectively.

3.2 Load–Displacement Curves

The load–displacement curves of the two test beams are shown in Fig. 10. The difference between the test beams in ultimate flexural load capacity was small, and the composite beam with pre-embedded angle connectors was higher. In the elastic–plastic phase, composite beams with angle connectors have higher flexural stiffness. After the bonding force failed, the pre-embedded angle and stud connectors functioned as shear connectors to improve the shear connection of the members. The angle connectors reduce the slippage between the concrete and the steel beam, allowing for better plasticity of the steel beam. Thus, the flexural load capacity of the member was improved, which was in accordance with other literature findings (Lv et al., 2020; Nie, 2005).

4 Finite Element Analysis

The use of finite element modeling to analyze the proposed connector can effectively save the cost and time required for full-scale experiments. In addition, the finite element analysis can predict the shear performance of the connection in flexural and push-out tests and obtain accurate simulation results (Nguyen & Kim, 2009). Therefore, Abaqus finite element software was used to simulate the tests.
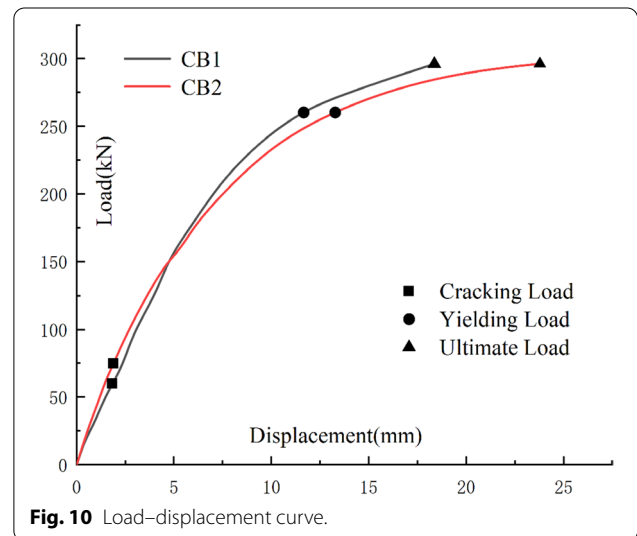

Fig. 10 Load–displacement curve.

Table 3 Main test results of specimens CB1 and CB2.

Specimen	P_{cr} (kN)	δ_{cr} (mm)	P_y (kN)	δ_y (mm)	P_u (kN)	δ_u (mm)
CB1	75	1.98	240.8	10.81	296.08	18.35
CB2	90	2.36	255.1	9.89	296	23.8

Ding *et al. Int J Concr Struct Mater*   (2022) 16:15

Page 8 of 16

4.1 Flexural Test Simulations

4.1.1 Material Properties

The concrete material properties were adopted from the concrete damage plasticity model in the software. This is a plasticity-based continuous media damage model that can be used for monotonic loading, cyclic loading. It is compatible with the loading regime of this test. The uniaxial tensile and compressive stress-strain curves and the tensile and compressive damage factor-elastic strain curves are simulated using the curves in Appendix C of the "Code for the Design of Concrete Structures" (GB50010-2010, 2010; Sun, 2014). Steel unidirectional stress–strain curve adopted a bi-linear model. The model is suitable for monotonic loading and the material property parameters were measured by intercepting the test steel.

4.1.2 Model Building

Fig. 11 shows the test model. The boundary conditions of the model were established according to the constraints of the simply supported beam. The loading method of displacement was adopted to load the member at the mid-span. In addition, concrete, angle connectors, stud connectors, and steel beams were simulated using C3D8R solid units (Lv et al., 2020; Nguyen & Kim, 2009). Rebars and reinforced trusses were simulated using T3D2 truss units. Set tie constraint between the precast slab and the cast-in-place slab. To prevent excessive restraint of the stud connectors, they were divided near the root along the height direction. The contact surface between the root of the stud connector and the steel beam was set as a tie constraint, and the upper part of the stud was embedded in the concrete slab. The shear resistance of the stud connectors was achieved by means of solid units at the roots, in accordance with the actual forces (Nie et al., 1996). In order to better simulate the actual working conditions, the weld seam of the angle connector was simulated by creating a chamfer. Set tie constraint between

the welded surface of the angle connector and the steel beam. To better simulate the actual working conditions, the concrete slab is pre-drilled for the angle connectors at the corresponding locations. The contact surface of the concrete and angle connectors adopted the contact interaction. In addition, the friction coefficient in the contact interaction was adopted as 0.25 (Ellobody et al., 2006).

4.1.3 Comparison of Simulation and Experiment

As shown in Fig. 12, the simulated load–displacement curves of the two composite beams were compared with the experimental results. The numerical simulation results of each group basically agree with the experimental results, but the stiffness of the load–displacement curve was slightly larger in the numerical simulation case. This might be due to the fact that the material is more homogeneous in the finite element software and the material properties are more desirable. During the test loading, the upper flange of the steel beam at the loading point buckled and lost its load-carrying capacity. As a result, the performance of the steel beam is not fully developed and the stiffness was lower than the theoretical value.

4.2 Push-Out Test Simulation

The pre-embedded angle connector designed in this paper has a different shear resistance than the stud connector. Its shear resistance has obvious directionality. Therefore, the shear resistance of this pre-embedded angle connector needs to be further investigated by transverse push-out tests. Based on the finite element model of the flexural test, the simulations of the transverse push-out test were conducted.

4.3 Material Properties

The concrete material properties used for the push-out test simulations were consistent with the above. In other scholars' studies, the angle connector was subjected to
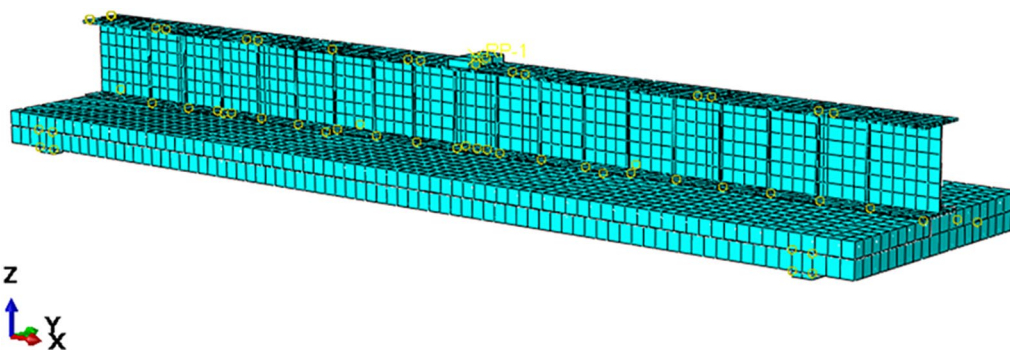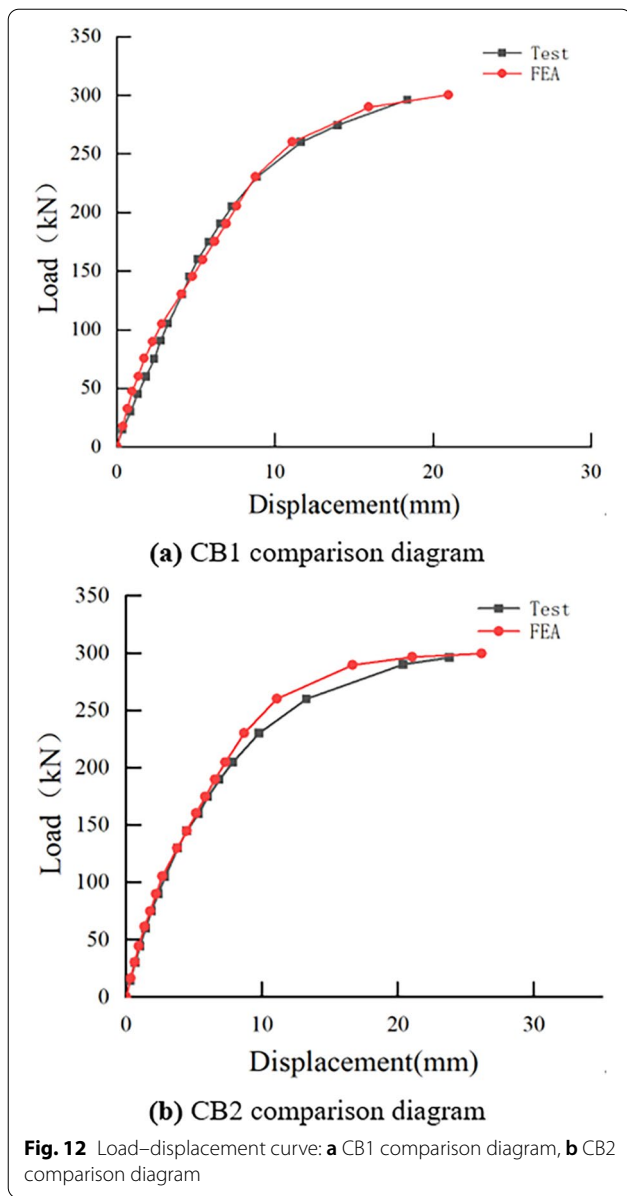

Fig. 11 Experimental model.

Ding *et al. Int J Concr Struct Mater*   (2022) 16:15

Page 9 of 16

Fig. 12 Load–displacement curve: **a** CB1 comparison diagram, **b** CB2 comparison diagram
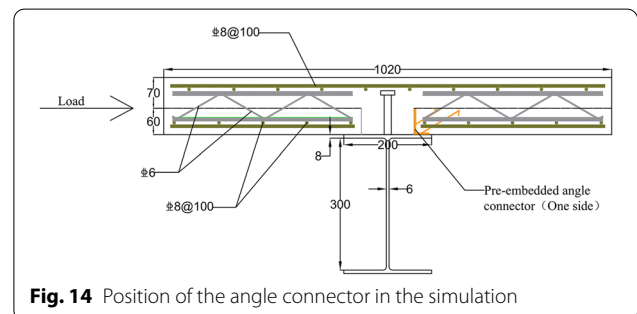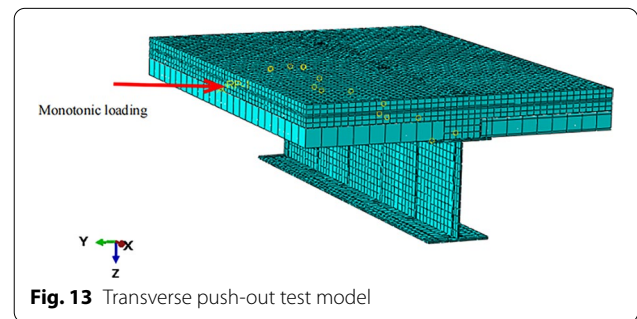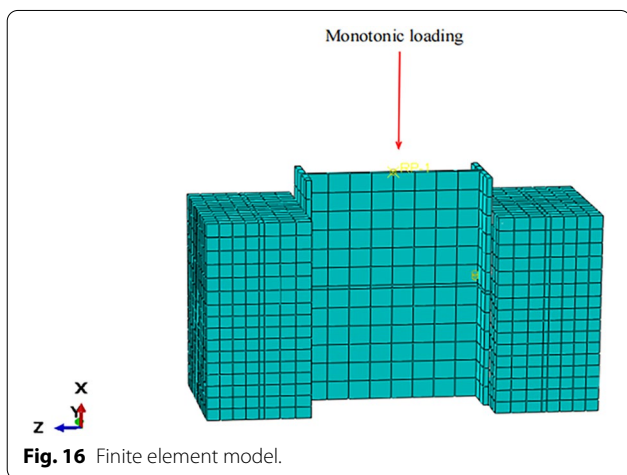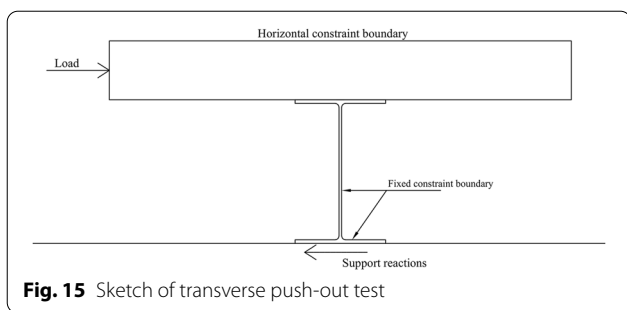
large plastic deformation or even shearing at both the root of the connector and the weld during the test (Qiu et al., 2021). As a result, shear damage and flexible damage in ABAQUS were used to simulate the degradation of the strength and stiffness of the angle connector (Liu, 2020). The rest of the steel material property models were consistent with the above.

4.4 Model Building

The standard push-out test in the Eurocode can be used to evaluate the shear strength of connectors (Johnson & Anderson, 2004). However, most of the studies are on the longitudinal shear resistance of connectors, which is

what this Eurocode method is aimed at. In this paper, the transverse shear strength of the connectors could not be tested by the standard push-out test. Therefore, this test setup is used to create a transverse shear resistance condition. The use of the transverse push-out test setup to test the transverse shear capacity is a supplement to the shear content of the composite beam. Fig. 13 shows the transverse push-out test model. To save the calculation cost, 1/3 part of the composite beam was taken for the simulation of the push-out test. The section of the composite beam for the transverse push-out test is the same size as the section of the composite beam for the negative moment test. The beam length is 1/3 of the original, which means that a simulated specimen has only 2 precast slabs and 4 angle connectors. Fig. 14 shows the position of the angles in the simulation. Since the angles are in opposite directions, only one side of the angle connectors were simulated to ensure the accuracy of the results. The simulation was conducted with the load applied in the direction perpendicular to the composite beam. And the position of the angle connectors in the simulation is parallel to the shear. The boundary conditions of horizontal constrain were applied to the surface of the slab to prevent buckling of the slab. To prevent the steel beam web from buckling in the simulation, the boundary conditions of fixed constrain were imposed on the lower flange and web of the steel beam (Li et al., 2017). The beam–concrete contact was set as surface-to-surface contact, the connector and the beam were set

Fig. 13 Transverse push-out test model

Fig. 14 Position of the angle connector in the simulation

Ding *et al. Int J Concr Struct Mater*   (2022) 16:15

Page 10 of 16

Fig. 15 Sketch of transverse push-out test

Fig. 16 Finite element model.

Fig. 17 Comparison of FEA analysis results and test results.

Table 4 Mahdi test results and simulation results.

Type	TEST (Shariati et al., 2013)	FEA
Failure load (kN)	109.6	108.9
Maximum slip (mm)	5.5	5.5

Table 5 Comparison of simulation results and calculation results.

Specimen	Size	P_u (kN)	$P_{n, AISC}$	P_u (kN)/$P_{n, AISC}$
FEM-6	L-50–32-4 ($t_f = 5$)	142.79	119.53	1.19
FEM-7	L-50–32-4 ($t_f = 6$)	154.35	136.61	1.13
FEM-8	L-50–32-4 ($t_f = 7$)	167.76	153.69	1.09
FEM-9	L-50–32-4 ($t_f = 8$)	175.7	170.76	1.03

as tie constraints, and the rebars were embedded in the concrete slab. The same contact interaction as above was used for the contact surfaces of the concrete and angle connectors. Fig. 15 shows the sketch of transverse push-out test. The web and lower flange of the steel beam are subjected to fixed constraints, which provide the support reactions when the load is transferred from the slab. At this stage, the load and the support reactions of the steel beam are the transverse shearing force of the composite beam.

4.5 Verification of Finite Element Model

To verify the correctness of the model, a set of tests by Mahdi et al. was simulated using Abaqus finite element software, then the simulations were compared with the experimental results. This test is a monotonic push-out test of a composite beam with angle connectors, which is consistent with the push-out test simulations studied in this paper (Shariati et al., 2013).

Fig. 16 shows a push-out simulation model of the Mahdi et al. experiment. The constraints and loads were set according to the experimental boundary conditions of Mahdi et al., which are similar to the transverse push-out test.
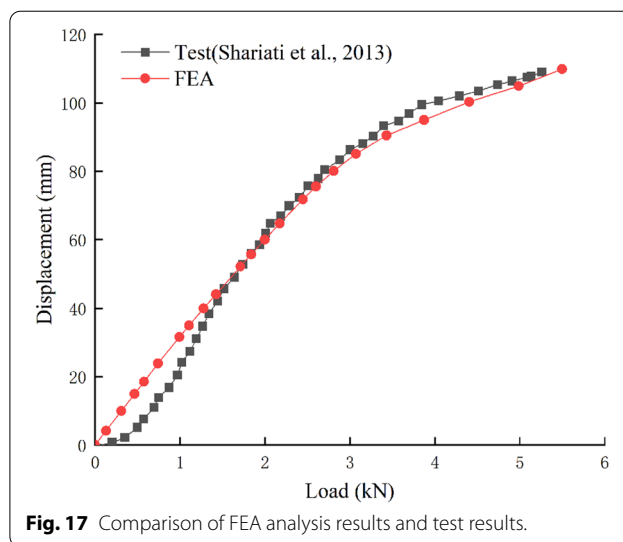
Fig. 17 shows a comparison of the FEA results and the test results. Table 4 shows the results of Mahdi's experiments and simulations. The test was taken from the Mahdi test in which A7550-M reached the failure load capacity stage (Shariati et al., 2013). The simulated initial stage stiffness was slightly higher than the test, and the later stage stiffness was slightly lower than the test. However, the above differences are within reasonable limits, and the Abaqus test results are in general agreement with the test. Therefore, the simulation was verified to be reasonable.

As shown in Table 5, P_u indicates the strength of the angle connector for the transverse push-out test, and $P_{n, AISC}$ represents the design value of the strength of the angle connector. The simulated values are larger than the calculated values because the design values are conservative. In addition, the ratios are within a reasonable range, which further verifies the validity of the simulations.

5 Strength of the Angle Connector

5.1 Existing Theoretical Research

At present, there is less research on the formula for calculating the shear resistance of angle connectors in China. Only a few scholars had investigated it by push-out experiments and proposed empirical equations (Zhou et al., 1994). And there is no unified strength design formula for angle connectors in China as a reference, and the forms of its strength design formulae differ in foreign countries (American Institute of Steel Construction, 2016; Canadian Standards Association, 2001). The yield strength of the angle connector was taken into account in the equation for Zhou (Zhou et al., 1994), but the flange thickness of the angle connector is not considered. The strength of the angle connector design equations from the American Institute of Steel Construction (AISC) and the Canadian Standards Association (CAN/CSA) are relatively similar. However, the formulas in the United States and Canada include the flange thickness of the angle connector, but not the yield strength. The following angle strength equations are taken from AISC, CAN/CSA, Zhou, respectively:

$$Q_{n,\text{AISC}} = 0.3(t_f + 0.5t_w)L_c\sqrt{f_c'E_c}, \tag{1}$$

$$Q_{n,\text{CAN/CSA}} = 36.5(t_f + 0.5t_w)L_c\sqrt{f_c'}, \tag{2}$$

$$Q_{\text{n,Zhou}} = \left(0.16t_W f_s + \frac{0.6t_W f_s}{1 + 0.15f_c'} + t_W f_c'\right)L_c, \tag{3}$$

where t_f is the thickness of the web of the angle connector, t_w means the flange thickness of the angle connector, f_s denotes the yield strength of the angle connector, f_c' refers to the compressive strength, L_c represents the length of the angle connector, and E_c is the modulus of elasticity of concrete. The yield strength of an angle connector indicates that a plastic strain will occur in the connector when the corresponding stress reaches that point.

5.2 Angle Connector Strength Design Equation

Based on the research of other scholars and combined with the experimental results, it is concluded that angle and channel connectors work similarly in composite beam (Zhou et al., 1994). The roots of the angle and channel connections are welded to the steel beam and the upper part is fixed in the concrete, which is equivalent to a beam fixed at both ends in the elastic phase. According to Vest's "elastic foundation beam" theory, the model assumes that the stiffness of the bottom flange of the connector is infinite (Viest, 1995). This is consistent with other scholars' tests, because the bottom flange was not

damaged but sheared off when most of the connectors were damaged (Shariati et al., 2020). In the elastic section, the connector bearing capacity is mainly achieved by the root shear. Since the stiffness of the connector is greater than the stiffness of the concrete. As the load increases, the concrete at the root of the connector fails first. It will not provide higher concrete reaction force as the load increases. In the plastic section, the connector bearing capacity is achieved by the angle shear and tensile, tensile force provides part of the shear force for the connector, resulting in the actual bearing capacity of the connector is larger than the shear load. In addition, because the channel connector has more upper flange than the angle connector, it can resist more tensile force, thus increasing its load capacity, which is consistent with the conclusions of other scholars (Shariati et al., 2020). Fig. 18 shows the model of the angle connector.

Fig. 19 shows a model of the peg connector. The studs can also be analyzed using the "beam on elastic foundation" model to obtain accurate results (Gelfi et al., 2002). As shown in the figure, the shear deformation of the studs can also be divided into elastic and plastic sections,
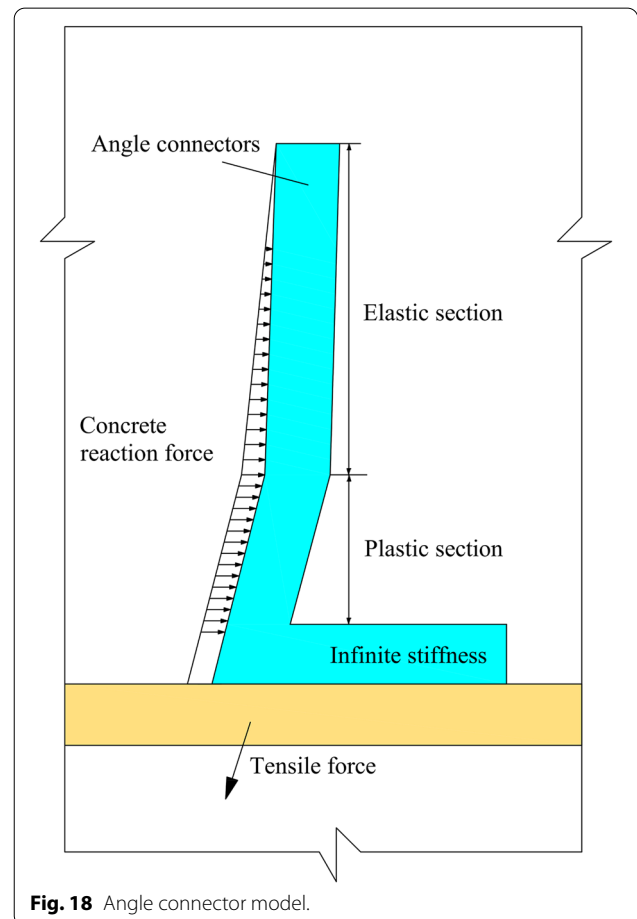

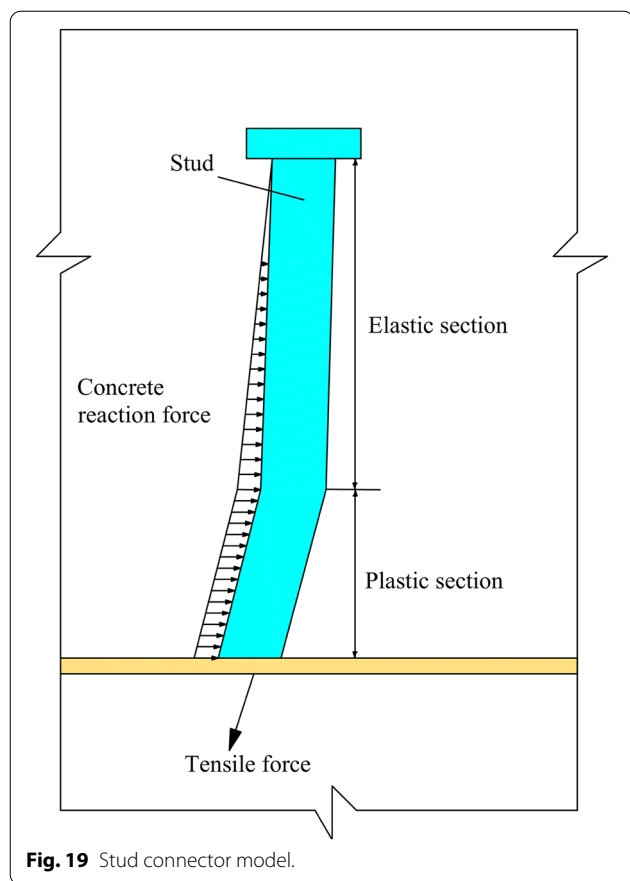**Fig. 18** Angle connector model.

Fig. 19 Stud connector model.

and the plastic zone will continue to elongate as the load increases.

In this paper, a pre-embedded angle connector with welded bent-up bars was proposed. According to the test observations and simulations, the shear bearing capacity also includes the shear resistance of the welded reinforcement, which is similar to the working principle of Hu PBL shear connectors. The shear resistance of reinforcement is linearly related to the product of its cross-sectional area and yield strength (Hu et al., 2006). Zhou's analysis of the experimental phenomena led to the conclusion that the angle and channel connectors in composite beams work in similar ways. The "beam on elastic foundation" model was introduced to analyze the shear bearing capacity of angle connectors, where the angle connectors accomplish shear work by local compression. Resistance to shear forces is mainly through the roots. When the member was damaged, part of the angle connector occurred a large plastic deformation. As a result, Zhou considered that the shear bearing capacity of the angle connector is related to its yield strength, without considering the flange thickness of the angle connector (Zhou et al., 1994). However, the AICS and CAN equations do not take into account the angle connector yield strength, and the shear strength is calculated considering the flange thickness of the angle connector. Based on this, parametric simulations were conducted for these two factors.

Table 6 shows a comparison between the theoretical values calculated using the design equations and the simulation results. Comparison of theoretical values calculated using design equations and simulations. As can be seen from the table, the difference between the calculated values of the AISC formula and the simulation results is not significant. The reliability of the simulation results is further illustrated by the fact that the ratios are very close, especially when the analysis of the flange thickness of the angle connector as a variable is performed. However, the AISC and CAN equations do not take into account the yield strength of the angle connector, and the calculated values of the shear bearing capacity were

Table 6 Comparison of the theoretical calculations and the simulated calculations.

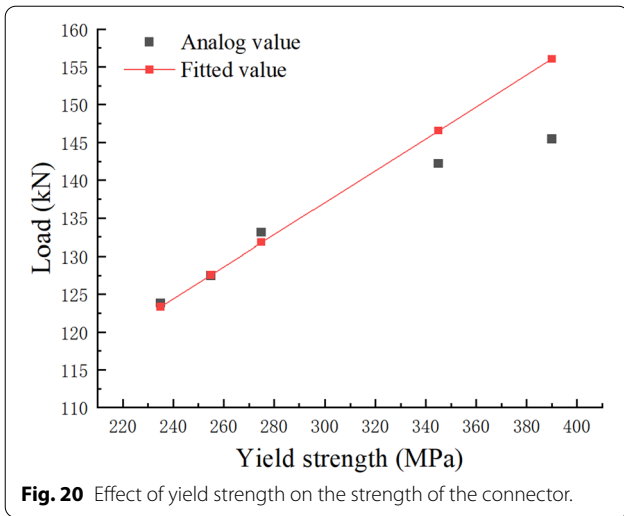|	Size	f_s (MPa)	P_u (kN)	$P_{n,AISC}$	$P_u/P_{n,AISC}$	$P_{n,CAN}$	$P_u/P_{n,CAN}$	$P_{n, Zhou}$	$P_u/P_{n,Zhou}$	$P_{n,New}$	$P_u/P_{n,New}$
FEW-1	$t_f=4$	235	123.86	102.45	1.21	71.97	1.72	29.09	4.2	123.33	1.00
FEW-2	$t_f=4$	255	127.47		1.24		1.76	30.77	4.14	127.55	0.99
FEW-3	$t_f=4$	275	133.07		1.3		1.85	32.45	4.1	131.77	1.01
FEW-4	$t_f=4$	345	142.2		1.38		1.98	38.32	3.71	146.56	0.97
FEW-5	$t_f=4$	390	145.45		1.42		2.02	42.1	3.45	156.06	0.93
FEW-6	$t_f=5$	345	142.79	119.53	1.19	83.97	1.7	44.62	3.73	150.86	0.95
FEW-7	$t_f=6$	345	154.35	136.61	1.13	95.96	1.61		4.03	155.16	0.99
FEW-8	$t_f=7$	345	167.76	153.69	1.09	107.96	1.55		4.38	159.47	1.05
FEW-9	$t_f=8$	345	175.7	170.76	1.03	119.95	1.46		4.59	163.77	1.07
Average					1.221		1.739		4.037		1.029
Standard deviation					0.130		0.188		0.355		0.047
Coefficient of variation					0.106		0.108		0.088		0.046

Fig. 20 Effect of yield strength on the strength of the connector.

constant at different strengths. This led to a large difference between the results and the simulated values. The calculated value of the Zhou formula was expanded by a factor of 1.3 when considering the load subfactor. Calculated results are still a large gap with the simulation results. In practical applications often make the material performance does not fully utilize. Based on this, the following equation was proposed through the nonlinear least squares method with the basic variables described below (Ahmad et al., 2020):

$$Q_{n,\,\text{New}} = \frac{97}{100,000}\left[0.78\sqrt{f_c'}L_c f_s\left(0.0488 t_f + 0.1577 t_w\right) + 3.3056 A_{tr} f_y\right].\tag{4}$$

The former half of the formula is the angle shear bearing capacity formula, and the latter half is the shear resistance of welded rebars, where t_f is the web thickness of the angle connector, t_w means the flange thickness of
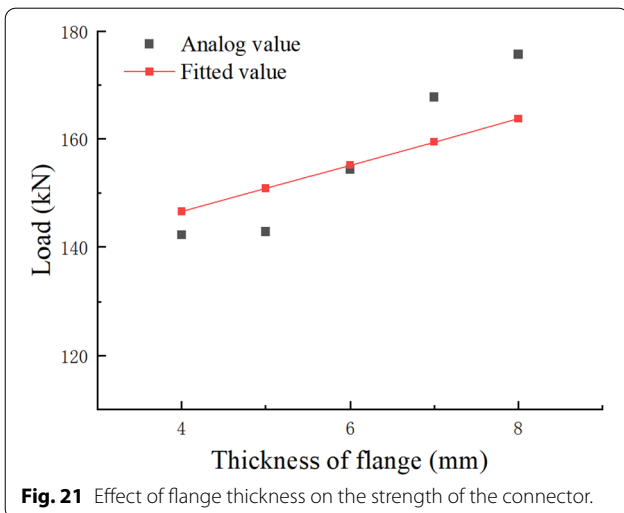

Fig. 21 Effect of flange thickness on the strength of the connector.

the angle connector, f_s denotes the yield strength of the angle connector, f_c' refers to the compressive strength, L_c means the length of the angle connector, A_{tr} is the modulus of elasticity of concrete, f_y indicates the yield strength of the welded reinforcement.

Figs. 20 and 21 show the effect of yield strength and flange thickness on the strength of an angle connector.

As shown in Table 6, the designed shear bearing capacity equation is highly accurate. The average value of the new formula is 1.029, and the standard deviation and coefficient of variation are also the smallest and closest, at 0.046 and 0.047, respectively. In addition, it means that this equation gives more accurate results than the AISC and CAN/CAS equations when it comes to calculating the strength of angled connectors.

6 Conclusions

In this paper, the strength and performance of the designed pre-embedded angle connectors were investigated through negative moment flexural tests and push-out test simulations of the composite beam. In addition, the equation is presented for the designed pre-embedded angle connectors. The results of this formula are more accurate than current specifications and research calculations. Besides, this equation is also practical for general angle connectors. Moreover, the necessity of considering the strength of the connector and the thickness of the connector flange was determined. These two variables are controversial in the study and the current codes. The following conclusions can be derived. However, this angle shear connection was only studied in steel–concrete composite beams and was not tested in other types of composite beams. In the situation of combined longitudinal–transverse response, it is important to understand how the connectors work and how they can be predicted. An in-depth study in these two areas is necessary and relevant. This would be further work.

(1) In the flexural test, the shear connection of the composite beam with angles is higher than that of the conventional composite beam with precast slabs. This results in increased stiffness of the specimen, reduced slip and little change in ultimate flexural load capacity.

(2) During the flexural test, no cracks were developed at the laminated faces of both composite beams. This shows that good overall performance can still be achieved for concrete slabs with angle connectors. In addition, precast slabs with angles are more

Ding *et al. Int J Concr Struct Mater*   (2022) 16:15

Page 14 of 16

convenient for the fabrication of composite beams than conventional precast slabs.

(3) According to the simulation results, the angle steel connectors proposed in this paper can provide a transverse shear capacity of 142.2 kN. When the main beams are far apart and the transverse connections are weak, the effect of improving the transverse shear capacity of the composite beams can be achieved by increasing the angle connectors of the precast slabs.

(4) The results illustrate that the strength of the angle connectors increases with the increase in yield strength and flange thickness of the connectors. Therefore, this paper proposed a new equation for the shear strength of angles based on the previous study. The standard deviation of the equation is 0.047, which indicates the feasibility of this equation.

Authors' information
KD is a professor at the School of Civil Engineering, Anhui Jianzhu University, Hefei, Anhui, China. XZ is a Master student from the School of Engineering, Anhui Jianzhu University, Hefei, Anhui, China. YL is a professor at the School of Civil Engineering, Anhui Jianzhu University, Hefei, Anhui, China. SH is a Master student from the School of Engineering, Anhui Jianzhu University, Hefei, Anhui, China. JW is a professor at the College of Civil Engineering, Hefei University of Technology, Hefei, Anhui, China. WS is a Vice President of Fuhuang Steel Structure, Hefei, Anhui, China.

Availability of data and materials
The datasets used and/or analyzed in this investigation are available upon reasonable request from the corresponding author.

Declarations

Competing interests
The authors declare that they have no competing interests in this paper.

Author details
[1]College of Civil Engineering, Anhui Jianzhu University, Hefei 230601, Anhui, China. [2]College of Civil Engineering, Hefei University of Technology, Hefei 230601, Anhui, China. [3]Anhui Fuhuang Steel Structure Co., Ltd, Hefei 230601, Anhui, China.

References

Ahmad, K., Qaiser, A., & Soori, A. H. (2020). Nonlinear least squares solutions of ordinary differential equations. *Mitteilungen Klosterneuburg, 70*(2), 53–67.

AISC 360-16. (2016). Specification for structural steel buildings. Chicago: American Institute of Steel Construction. https://www.aisc.org/globalassets/aisc/publications/standards/a360-16-spec-and-commentary.pdf. Accessed 20 Oct 2021.

CAN/CSA S16-01. (2001). Limit States Design of Steel Structures. Canadian Standards Association. https://www.techstreet.com/products/preview/1098669. Accessed 20 Oct 2021.

Chahnasir, E. S., Zandi, Y., Shariati, M., Dehghani, E., Toghroli, A., Mohamad, E. T., Shariati, A., Safa, M., Wakil, K., & Khorami, M. (2018). Application of support vector machine with firefly algorithm for investigation of the factors affecting the shear strength of angle shear connectors. *Smart Structures and Systems, 22*(4), 413–424. https://doi.org/10.12989/sss.2018.22.4.413

Ellobody, E., Young, B., & Lam, D. (2006). Behaviour of normal and high strength concrete-filled compact steel tube circular stub columns. *Journal of Constructional Steel Research, 62*(7), 706–715. https://doi.org/10.1016/j.jcsr.2005.11.002

Ding, K., Chen, D., Liu, Y. L., & Xia, S. (2015). Theoretical and experimental study on mechanical behavior of laminated slabs with new type joints. *China Civil Engineering Journal, 48*(10), 64–69. https://doi.org/10.15951/j.tmgcxb.2015.10.009

Ding, K., Ye, Y., & Ma, W. (2021). Seismic performance of precast concrete beam-column joint based on the bolt connection. *Engineering Structures, 232*, 111884. https://doi.org/10.1016/j.engstruct.2021.111884

Davoodnabi, S. M., Mirhosseini, S. M., & Shariati, M. (2019). Behavior of steel-concrete composite beam using angle shear connectors at fire condition. *Steel and Composite Structures, 30*(2), 141–147. https://doi.org/10.12989/scs.2019.30.2.141

Davoodnabi, S. M., Mirhosseini, S. M., & Shariati, M. (2021). Analyzing shear strength of steel-concrete composite beam with angle connectors at elevated temperature using finite element method. *Steel and Composite Structures, 40*(6), 853–868. https://doi.org/10.12989/scs.2021.40.6.853

Gelfi, P., Giuriani, E., & Marini, A. (2002). Stud shear connection design for composite concrete slab and wood beams. *Journal of Structural Engineering, 128*(12), 1544–1550. https://doi.org/10.1061/(ASCE)0733-9445(2002)128:12(1544)

GB/T 706–2016, (2016). Hot rolled section steel. China Building Industry Press. http://www.jianbiaoku.com/webarbs/book/94533/3062376.shtml. Accessed 20 October 2021.

GB/T 10433-2002. (2002). Cheese head studs for arc stud welding. China Building Industry Press. http://www.jianbiaoku.com/webarbs/book/11933/556491.shtml. Accessed 20 Oct 2021.

GB 50010-2010.(2010). Code for design of concrete structures. China Building Industry Press. http://www.jianbiaoku.com/webarbs/book/209/2438396.shtml. Accessed 20 Oct 2021.

GB 50152-2012. (2012). Standard for test method of concrete structures. China Building Industry Press. http://www.jianbiaoku.com/webarbs/book/224/2296382.shtml. Accessed 20 Oct 2021.

GB 50017-2017. (2017). Standard for design of steel structures. China Building Industry Press. http://www.jianbiaoku.com/webarbs/book/198/3733703.shtml. Accessed 20 Oct 2021.

GB/T 228.1-2010. (2010). Metallic materials- tensile testing-part 1: method of test at room temperature. China Building Industry Press. http://www.jianbiaoku.com/webarbs/book/12352/450113.shtml. Accessed 20 Oct 2021.

Hu, J. H., Ye, M. X., & Huang, Q. (2006). Experiment on bearing capacity of PBL shear connectors. *China Journal of Highway and Transport, 19*(6), 65–72. https://doi.org/10.19721/j.cnki.1001-7372.2006.06.013

Huang, H., Yuan, Y., Zhang, W., & Zhu, L. (2021). Property assessment of high-performance concrete containing three types of fibers. *International Journal of Concrete Structures and Materials, 15*(1), 39. https://doi.org/10.1186/s40069-021-00476-7

JTG/T D64-01-2015, (2015). *Specifications for design and construction of highway steel-concrete composite Bridges*. China Communications Press. http://www.jianbiaoku.com/webarbs/book/80111/2935854.shtml. Accessed 20 Oct 2021.

Johnson, R. P., & Anderson, D. (2004). *Designers' Guide to EN 1994–1–1: Eurocode 4: Design of Composite Steel and Concrete Structures*. General Rules and

Rules for Buildings. Thomas Telford. https://eurocodes.jrc.ec.europa.eu/showpage.php?id=134. Accessed 20 Oct 2021.

Li, J., Si, P. Z., Guo, W. F., & Jiang, L. (2017). Study on the seismic performance for joints of reinforced concrete superposed slab and steel girder. *Structural Engineers, 33*(03), 166–173. https://doi.org/10.15935/j.cnki.jggcs.2017.03.021

Liu, Y., Guo, L., Qu, B., & Zhang, S. (2017). Experimental investigation on the flexural behavior of steel-concrete composite beams with U-shaped steel girders and angle connectors. *Engineering Structures, 131*, 492–502. https://doi.org/10.1016/j.engstruct.2016.10.037

Liu, X. (2017). Analysis of flexural performance of steel-precast ribbed concrete composite beams. Master, Shandong University. https://kns.cnki.net/kcms/detail/detail.aspx?dbcode=CMFD&dbname=CMFD201702&filename=1017069015.nh&uniplatform=NZKPT&v=Qo%5mmd2FtlFm1G8wfLNwy6w9pfo96Z9B4MVCfqC%5mmd2FcSO1h%5mmd2FEFaoFFBrH1F4%5mmd2F1j3DFjqPDY. Accessed 20 Oct 2021.

Liu, Y. (2020). Flexural behaviour and fire resistance of composite beams with U-shaped steel girder and angle connectors. Harbin Institute of Technology. https://r.cnki.net/Kreader/CatalogViewPage.aspx?dbCode=CDFD&filename=1020401577.nh&tablename=CDFDLAST2021&compose=&first=1&uid=&ecode=CDFD. Accessed 20 Oct 2021.

Liu, Y. L., Ding, K. W., Ye, X. G., Yin, W. Y., & Chong, X. (2014). Experimental study of load transfer behavior of reinforced joints between superimposed slabs. *Industrial Building, 44*(05), 49–51. https://doi.org/10.13204/j.gyjz201405011

Lv, J. L., Zhou, S. N., Lv, J. J., Cai, Y. Y., & Chen, Q. C. (2020). Experimental and simulation study on mechanical properties of separated composite beam with laminated slabs. *Journal of Shandong Jianzhu University, 35*(04), 11–17. https://doi.org/10.12077/sdjz.2020.04.002

Nguyen, H. T., & Kim, S. E. (2009). Finite element modeling of push-out tests for large stud shear connectors. *Journal of Constructional Steel Research, 65*(10–11), 1909–1920. https://doi.org/10.1016/j.jcsr.2009.06.010

Nie, J. G., Shen, J. M., Yuan, Y. S., Lin, W., & Wang, W. H. (1996). Experiment and analysis of actual shear capacity of shear connectors in composite steel-concrete beams. *Journal of Building Structures, 17*(02), 21–28.

Nie, J. G., & Yu, Z. W. (1999). Research and practice of composite steel-concrete beams in china. *China Civil Engineering Journal, 32*(2), 3–8. https://doi.org/10.3321/j.issn:1000-131X.1999.02.001

Nie, J. G., Chen, B. L., Chen, G., Guo, Z. G., & Wei, J. (2003). Experimental study on shear behavior of rc laminated slabs. *Industrial Construction, 33*(12), 43–46. https://doi.org/10.3321/j.issn:1000-8993.2003.12.014

Nie, J. G. (2005). *Steel-concrete composite beam structure: Experiment, theory and application*. Science Press.

Nouri, K., Sulong, N. R., Ibrahim, Z., & Shariati, M. (2021). Behaviour of novel stiffened angle shear connectors at ambient and elevated temperatures. *Advanced Steel Construction, 17*(1), 28–38. https://doi.org/10.18057/IJASC.2021.17.1.4

Paknahad, M., Shariati, M., Sedghi, Y., Bazzaz, M., & Khorami, M. (2018). Shear capacity equation for channel shear connectors in steel-concrete composite beams. *Steel and Composite Structures, 28*(4), 483–494. https://doi.org/10.12989/SCS.2018.28.4.483

Qiu, S. Y., Fan, J. S., Nie, J. G., Tang, L., Song, S. Y., & Xu, G. P. (2021). Experimental and theoretical study on shear stiffness of angle shear connectors. *China Journal of Highway and Transport, 34*(3), 136–146. https://doi.org/10.19721/j.cnki.1001-7372.2021.03.009

Safa, M., Shariati, M., Ibrahim, Z., Toghroli, A., Baharom, S. B., Nor, N. M., & Petkovic, D. (2016). Potential of adaptive neuro fuzzy inference system for evaluating the factors affecting steel-concrete composite beam's shear strength. *Steel and Composite Structures, 21*(3), 679–688. https://doi.org/10.12989/scs.2016.21.3.679

Sahu, S. K., & Das, P. (2020). Experimental and numerical studies on vibration of laminated composite beam with transverse multiple cracks. *Mechanical Systems and Signal Processing, 135*(1), 106398. https://doi.org/10.1016/j.ymssp.2019.106398

Sedghi, Y., Zandi, Y., Shariati, M., Ahmadi, E., Azar, V. M., Toghroli, A., Safa, M., Mohamad, E. T., Khorami, M., & Wakil, K. (2018). Application of ANFIS technique on performance of C and L shaped angle shear connectors. *Smart Structures and Systems, 22*(3), 335–340.

Shariati, A., Sulong, N. H., Suhatril, M., & Shariati, M. (2012). Investigation of channel shear connectors for composite concrete and steel T-beam.

International Journal of the Physical Sciences. https://doi.org/10.5897/IJPS11.1604

Shariati, M., Ramli Sulong, N. H., Sinaei, H., Arabnejad Khanouki, M. M., & Shafigh, P. (2010a). Behavior of channel shear connectors in normal and light weight aggregate concrete (experimental and analytical study). *Advanced Materials Research, 168–170*, 2303–2307. https://doi.org/10.4028/www.scientific.net/AMR.168-170.2303

Shariati, M., Ramli Sulong, N. H., & Arabnejad Khanouki, M. M. (2010b). *Experimental and analytical study on channel shear connectors in light weight aggregate concrete*. In Proceedings of the 4th international conference on steel composite structures (pp. 21–23).

Shariati, M., Ramli Sulong, N. H., & Arabnejad Khanouki, M. M. (2011a). Shear resistance of channel shear connectors in plain, reinforced and light-weight concrete. *Science of Research Essays, 6*(4), 977–963. https://doi.org/10.5897/SRE10.1120

Shariati, M., Ramli Sulong, N. H., Arabnejad Khanouki, M. M., & Shariati, A. (2011b, August). Experimental and numerical investigations of channel shear connectors in high strength concrete. In Proceedings of the 2011 world congress on advances in structural engineering and mechanics (ASEM'11+).

Shariati, M., Ramli Sulong, N. H., & Arabnejad Khanouki, M. M. (2012). Experimental assessment of channel shear connectors under monotonic and fully reversed cyclic loading in high strength concrete. *Materials & Design, 34*, 325–331. https://doi.org/10.1016/j.matdes.2011.08.008

Shariati, M., Ramli Sulong, N. H., Suhatril, M., Shariati, A., Arabnejad Khanouki, M. M., & Sinaei, H. (2013). Comparison of behaviour between channel and angle shear connectors under monotonic and fully reversed cyclic loading. *Construction and Building Materials, 38*, 582–593. https://doi.org/10.1016/j.conbuildmat.2012.07.050

Shariati, M., Shariati, A., Ramli Sulong, N. H., Suhatril, M., & Arabnejad Khanouki, M. M. (2014). Fatigue energy dissipation and failure analysis of angle shear connectors embedded in high strength concrete. *Engineering Failure Analysis, 41*, 124–134. https://doi.org/10.1016/j.engfailanal.2014.02.017

Shariati, M., Ramli Sulong, N. H., Shariati, A., & Kueh, A. B. H. (2016a). Comparative performance of channel and angle shear connectors in high strength concrete composites: An experimental study. *Construction and Building Materials, 120*, 382–392. https://doi.org/10.1016/j.conbuildmat.2016.05.102

Shariati, M., Sulong, N. R., Shariati, A., & Khanouki, M. A. (2016b). Behavior of V-shaped angle shear connectors: Experimental and parametric study. *Materials and Structures, 49*(9), 3909–3926. https://doi.org/10.1617/s11527-015-0762-8

Shariati, M., Toghroli, A., Jalali, A., & Ibrahim, Z. (2017). Assessment of stiffened angle shear connector under monotonic and fully reversed cyclic loading. In Proceedings of the 5th International Conference on Advances in Civil, Structural and Mechanical Engineering-CSM. http://doi.org/https://doi.org/10.15224/978-1-63248-132-0-44.

Shariati, M., Mafipour, M. S., Mehrabi, P., Bahadori, A., Zandi, Y., Salih, M. N., & Poi-Ngian, S. (2019). Application of a hybrid artificial neural network-particle swarm optimization (ANN-PSO) model in behavior prediction of channel shear connectors embedded in normal and high-strength concrete. *Applied Sciences, 9*(24), 5534. https://doi.org/10.3390/app9245534

Shariati, M., Tahmasbi, F., Mehrabi, P., Bahadori, A., & Toghroli, A. (2020). Monotonic behavior of C and L shaped angle shear connectors within steel-concrete composite beams: An experimental investigation. *Steel and Composite Structures, 35*(2), 237–247. https://doi.org/10.12989/SCS.2020.35.2.237

Shariati, M., Davoodnabi, S. M., Toghroli, A., Kong, Z., & Shariati, A. (2021). Hybridization of metaheuristic algorithms with adaptive neuro-fuzzy inference system to predict load-slip behavior of angle shear connectors at elevated temperatures. *Composite Structures, 278*, 114524. https://doi.org/10.1016/j.compstruct.2021.114524

Shariati, M., Mafipour, M. S., Mehrabi, P., Shariati, A., Toghroli, A., Trung, N. T., & Salih, M. N. A. (2021). A novel approach to predict shear strength of tilted angle connectors using artificial intelligence techniques. *Engineering with Computers, 37*(3), 2089–2109. https://doi.org/10.1007/s00366-019-00930-x

Shahabi, S. E. M., Sulong, N., Shariati, M., Mohammadhassani, M., & Shah, S. N. R. (2016). Numerical analysis of channel connectors under fire and a comparison of performance with different types of shear connectors

Ding *et al. Int J Concr Struct Mater*   *(2022) 16:15*

Page 16 of 16

subjected to fire. *Steel and Composite Structure, 20*(3), 651–669. https://doi.org/10.12989/scs.2016.20.3.651

Sun, Q. Z. (2014). An overview of plastic damage model of ABAQUS concrete. *Chongqing Architecture, 13*(11), 70–72. https://doi.org/10.3969/j.issn.1671-9107.2014.11.070

Toghroli, A., Mohammadhassani, M., Suhatril, M., Shariati, M., & Ibrahim, Z. (2014). Prediction of shear capacity shear connectors using the ANFIS model. *Steel and Composite Structures, 17*(5), 623–639. https://doi.org/10.12989/SCS.2014.17.5.623

Viest, I. M. (1951). Full-scale tests of channel shear connectors and composite t-beams. University of Illinois at Urbana Champaign, College of Engineering. Engineering Experiment Station. http://hdl.handle.net/2142/4365.

Zhou, W. D., Bai, J. N., Lei, Y. T., & Wang, X. Y. (1994). Experimental study on lattice push-out of angle steel connector ─ on the series of steel-concrete composite trusses part four. *Journal of Hefei University of Technology (natural Science), 02*, 126–130.

Publisher's Note